Title: Determinants of Protein-Level Parameters Governing MS2 Virus-Like Particles Reassembly

Authors: Daniel de Castro Assumpcao[1], Emma S. Vinokour[2], Madeline M. Mills[1], Shiqi Liang[3], Carolyn E. Mills[4], Aline Carvalho da Costa[5], Nolan W. Kennedy[1], Danielle Tullman-Ercek[1,*]

Affiliations: [1]Department of Chemical and Biological Engineering, Northwestern University, Evanston, Illinois, USA

[2]Weinberg College of Arts and Sciences, Northwestern University, Evanston, Illinois, USA

[3]Interdisciplinary Biological Sciences Program, Northwestern University, Evanston, Illinois, USA

[4]Department of Bioengineering, University of California, Santa Barbara, California, USA

[5]School of Chemical Engineering, University of Campinas, Campinas, Sao Paulo, Brazil

***** Corresponding author: 2145 Sheridan Road, Silverman 3619, Evanston, IL 60208; ercek@northwestern.edu. **Fax:** 847-491-3728. **Phone:** 847-491-7043.

Running title: Reassembly of MS2 Protein Nanoparticles

Pages: 34

Supplementary material pages: 12

Figures: 4

Supplementary material description:

Supplemental Information 1 summarizes literature on MS2 VLP disassembly/reassembly conditions. Supplemental Information 2 compares linearity across protein quantification methods. Supplemental Information 3 provides supporting calculations for statistical design of experiments using reassembly yield as the response.

Keywords: Capsid assembly, design of experiments, self-assembly, VLP

Abbreviations:

ANOVA: Analysis of Variance

BCA: Bicinchoninic Acid Assay

CP: Coat Protein

DOE: Design of Experiments

HPLC: High Performance Liquid Chromatography

SDS-PAGE: Sodium Dodecyl Sulfate-Polyacrylamide Gel Electrophoresis

SEC: Size Exclusion Chromatography

TEM: Transmission Electron Microscopy

TMAO: Trimethylamine N-Oxide

UV-Vis: Ultraviolet-Visible light spectrum

VLP: Virus-Like Particle

Abstract:

MS2 virus-like particles (VLPs) are widely used for nanotechnology and therapeutic delivery. While cargo is typically loaded into VLPs by disassembling the protein shell and reassembling it around a cargo of interest, protocols for disassembly and reassembly remain inconsistent and poorly standardized. Here we systematically assess a wide array of reported techniques and evaluate the key steps of this process experimentally. First, we optimize acid-based disassembly and acid removal methods and identify trade-offs between speed, recovery, and accessibility. Next, we examine what experimental conditions impact the VLP reassembly yield. We establish a standardized reassembly yield quantification framework using size exclusion chromatography calibrated against purified VLP standards. We then employ this framework in a full-factorial design of experiments that reveal that an increase in sodium chloride concentration strongly inhibits reassembly efficiency, while pH and crowding agents exert only minor effects. The linear model fits the experimental data indicates that optimal reassembly conditions extend beyond those tested to date. Our findings provide practical guidelines and a reproducible framework for MS2 VLP disassembly and reassembly, enabling more reliable encapsulation strategies across applications.

Introduction

The MS2 virus-like particle (VLP) is a protein-based nanoparticle derived from the capsid of the male-specific bacteriophage MS2 (*Emesvirus zinderi*) (Callanan et al., 2021). Composed solely of 180 identical copies of a 129-amino acid coat protein (CP), the MS2 VLP assembles into a 27 nm icosahedral structure that lacks viral RNA and is non-infectious (Golmohammadi, Valegård, Fridborg, & Liljas, 1993; Strauss & Sinsheimer, 1963). These protein nanoparticles can be readily produced in *Escherichia coli* using plasmid-based expression systems, where the expressed CPs spontaneously self-assemble around RNA molecules, including their encoding mRNA during translation (Hartman et al., 2018). Owing to their simplicity, symmetry, and genetic tractability, MS2 VLPs have become a widely used model in virology and a versatile platform in nanotechnology. They have been extensively investigated for applications in imaging, diagnostics, vaccination, and targeted drug delivery (Frietze, Peabody, & Chackerian, 2016; Fu & Li, 2016; Ikwuagwu & Tullman-Ercek, 2022). In therapeutic delivery, a common strategy involves disassembling the capsid to remove encapsulated bacterial RNA ("native" cargo), followed by reassembly in a buffered solution containing the cargo of interest resulting in a protein-based nanoparticle loaded with a desired molecule (Aanei, Glasgow, Capehart, & Francis, 2018; Ashley et al., 2011; A. Williams, Neophytou, F. Garmann, Chakrabarti, & N. Manoharan, 2024; Garmann, Goldfain, & Manoharan, 2019; Glasgow, Capehart, Francis, & Tullman-Ercek, 2012; Rolfsson et al., 2008; Stockley et al., 2007; Sugiyama, Hebert, & Hartman, 1967; Wu, Brown, & Stockley, 1995; Yang et al., 2024; Zhang et al., 2015; Zhou et al., 2025). Despite the widespread use of this approach, methodological details often vary considerably across studies, and researchers seldom report standardized metrics for evaluating reassembly efficiency. As a result, a standardized

method for MS2 disassembly/reassembly, as well as proper reassembly yield estimations, have yet to be formalized.

Some alternative strategies avoid disassembly altogether, relying instead on *in vivo* expression systems to alter the cargo (Pasloske, Walkerpeach, Obermoeller, Winkler, & DuBois, 1998), in vivo cargo conjugation to the interior of the VLP (Liang et al., 2025), or cargo replacement without disassembling the VLP (Szyszka et al., 2025). Nevertheless, the predominant *in vitro* protocol for cargo loading involves four main steps: (1) disassembling the MS2 VLP using acidic conditions to generate free coat protein, (2) removing the encapsulated native mRNA, (3) adjusting the pH of the coat protein solution, and (4) incubating the coat proteins with the target cargo under reassembly conditions (**Figure 1**). Despite the widespread use of this general framework, the specific conditions used in each step vary widely across studies. For example, incubation time and acid concentration during disassembly differ significantly (e.g. 30 min to 2 h), and reassembly conditions, such as buffer composition, pH, and the inclusion of crowding agents or salts, also lack standardization. Moreover, few publications clearly define or quantify reassembly yield, making it difficult to compare reassembly efficiencies across different protocols or draw conclusions from the existing literature (see **Supplemental Information 1** for an extensive comparison between experimental conditions across literature).

In this study, we systematically investigate each step of the *in vitro* cargo-loading process for MS2 VLPs, with a focus on the protein-level parameters and solution conditions that influence disassembly and reassembly. First, we examine how variations in acid incubation time affect the removal of native RNA. We then discuss alternative methods for adjusting the pH of the coat protein solution post-disassembly. Next, we evaluate current approaches for calculating reassembly yield and propose improved metrics for standardization. Finally, we implement a

statistical design of experiments (DOE) framework to simultaneously assess the effects of buffer pH, ionic strength, protein concentration, and molecular crowding on reassembly efficiency. Through this comprehensive analysis, we highlight the strengths and limitations of commonly used methods and propose standardized conditions for MS2 VLP disassembly and reassembly. We also offer practical recommendations for calculating and reporting reassembly yield to facilitate reproducibility and cross-study comparisons.

Results and Discussion

Incubation time with acetic acid impacts native cargo removal during disassembly

The first step in loading non-native cargo into MS2 VLPs involves disassembling the capsid and removing encapsulated native RNA using glacial acetic acid. Here, the acid serves two purposes: to disassemble the VLP and to precipitate its native nucleic acid cargo. Most published protocols employ a 2:1 volumetric ratio of glacial acetic acid to VLP solutions with VLPs typically at 10 mg/mL (Aanei et al., 2018; A. Williams et al., 2024; Garmann et al., 2019; Glasgow et al., 2012; Stockley et al., 2007, 2007; Sugiyama et al., 1967; Wu et al., 1995; Yang et al., 2024; Zhang et al., 2015; Zhou et al., 2025). However, some studies report using a 3:1 ratio (Ashley et al., 2011) or lower VLP concentrations (e.g., 4 mg/mL) (Zhang et al., 2015). Among the reported parameters, incubation time varies the most significantly across literature, from 30 min (Aanei et al., 2018; A. Williams et al., 2024; Glasgow et al., 2012; Wu et al., 1995; Yang et al., 2024; Zhang et al., 2015; Zhou et al., 2025) to 2 h (Ashley et al., 2011) (**Supplemental Information 1**). To identify optimal conditions for VLP disassembly, we considered the three primary goals of this step: (1) complete dissociation of the capsid into coat protein subunits, (2) efficient precipitation and removal of the encapsulated native RNA, and (3) maximum possible coat protein concentration

after disassembly. This last goal (maximum coat protein concentration) enables the choice of a wider range of initial coat protein concentrations in reassembly reactions.

To determine whether the lowest reported acetic acid-to-VLP ratio (2:1 v/v) and the highest reported VLP concentration (10 mg/mL) are sufficient for complete capsid disassembly, we analyzed samples before acid treatment and after acid treatment followed by centrifugation using size-exclusion chromatography (SEC) and transmission electron microscopy (TEM) (**Figure 2A–B**). The shift in SEC retention time from 8.1 min (intact capsid) to 14.0 min (disassembled protein) and the absence of intact particles in TEM micrographs indicate that these conditions fully disassemble the capsids. We confirmed protein integrity preservation after disassembly with sodium dodecyl sulfate–polyacrylamide gel electrophoresis (SDS–PAGE) (**Figure 2C**).

In addition to disassembling the capsid, the low pH generated by glacial acetic acid also promotes spontaneous precipitation of the native RNA packaged within MS2 VLPs. Efficient removal of this RNA is a critical step in the disassembly–reassembly process, as residual negatively charged nucleic acids can trigger unintended, premature self-assembly during pH neutralization, prior to the introduction of the desired cargo. A simple diagnostic metric to confirm the removal of nucleic acids from VLP is the ultraviolet-visible spectroscopy (UV-Vis) absorbance profiles, particularly ratio between absorbances at 260 nm and 280 nm. Pure RNA has an A_{260}/A_{280} of approximately 2.1 and pure proteins have an A_{260}/A_{280} of approximately 0.6. These values are heuristic with widespread use in the field, rather than a theoretical value and thus, may change according to the molecule composition. For MS2, we observe a drop in the A_{260}/A_{280} ratio of samples pre-disassembly (A_{260}/A_{280} ~1.65) and post-disassembly followed by centrifugation (A_{260}/A_{280} ~0.65), suggesting removal of the native cargo (**Figure 2A**). As noted by Garmann,

Goldfain, & Manoharan (2019), the clarified coat protein solution should ideally have an A_{260}/A_{280} ratio below 0.67 — preferably closer to 0.60 — to confirm effective removal of RNA.

Nucleic acid precipitation is driven by its protonation under acidic conditions, which decreases its solubility and enables nucleic acid separation from protein through standard solid–liquid separation techniques. While a single step centrifugation is used by all the consulted references, there is no consensus in the operational conditions (**Supplemental Information 1**). We tested only one condition, in which centrifugation for 15 min at 17,000 × *g* and 4 °C was sufficient to pellet nucleic acids and achieve an A_{260}/A_{280} = 0.65. Centrifugation followed by filtration could also be employed if the filter material is compatible with glacial acetic acid. Chromatography should be avoided as passing insoluble material through a column can cause clogging and reduce column lifespan.

To assess the impact of VLP-acetic acid incubation time on RNA removal, we measured A_{260}/A_{280} values following disassembly of 10 mg/mL VLPs in a 2:1 acetic acid solution across varying incubation durations. Our results show that a 90-min incubation consistently produces coat protein solutions with A_{260}/A_{280} ratios below 0.65, suggesting efficient RNA removal and optimal conditions for downstream reassembly (**Figure 2D**). Since not all laboratories have access to identical equipment, acid incubation time and centrifugation operational conditions should be tailored to specific experimental setups to ensure that this ratio approaches the ideal value of 0.60. It is also important to note that very high protein concentrations (>30 mg/mL) may lead to coat protein loss due to aggregation and should be tested prior to establishing internal protocols.

Once the capsid is disassembled and the native nucleic acid is removed, the next step is to eliminate the excess acetic acid. Common methods reported in the literature include desalting columns (Aanei et al., 2018; Glasgow et al., 2012; Wu et al., 1995; Yang et al., 2024; Zhou et al.,

2025) , dialysis (Ashley et al., 2011; Sugiyama et al., 1967; Zhang et al., 2015), and centrifugal filtration (A. Williams et al., 2024, 2024), each with distinct advantages and limitations. Centrifugal filtration is the fastest and most cost-effective approach but is also labor-intensive and can promote premature protein aggregation, especially if local protein concentrations become high near the filter membrane. Desalting columns offer an alternative approach and can be operated via either high-performance or gravity flow liquid chromatography. While high-performance liquid chromatography allows for higher precision, it requires capital equipment that may not be accessible in all settings. Gravity-based desalting is simple and accessible but can lead to protein loss due to residual acidity, as some collected fractions may retain low pH values due to the non-automated nature of the technique and thus should be excluded from reassembly steps. Dialysis offers the highest protein recovery at a reassembly-compatible pH, is straightforward to perform, and is inexpensive; however, it is the most time-consuming method. Overall, each of these approaches is acceptable for acetic acid removal, and the optimal choice depends on laboratory constraints such as available resources, equipment, and desired throughput. In this work, we adopted dialysis to maximize protein recovery and ensure precise pH control of the coat protein solution prior to reassembly.

Another critical variable in this buffer exchange step is the choice of buffer. An effective buffer should maintain the coat proteins in a disassembled and soluble state, prevent precipitation, and avoid introducing components that interfere with downstream reassembly. Most studies recommend acetic acid solutions ranging from 1 mM (pH ~4.4) to 20 mM (pH ~3.7). For example, Ashley et al., 2011 employed a 10 mM acetic acid buffer supplemented with 50 mM sodium chloride. While sodium chloride can enhance protein solubility, its effect on disassembled coat proteins remains unclear. Excess ionic strength may promote premature capsid reassembly in the

absence of cargo, thereby reducing encapsulation efficiency. For this reason, we use a 1 mM acetic acid solution with no salts as a dialysis buffer. The impact of salt concentration on reassembly efficiency is addressed in detail below.

Methods for determining reassembly yield and cargo impact on quantification

Before reassembly conditions can be optimized, reliable and standardized methods for quantifying reassembly yield must be established. Because reassembly rarely reaches 100% efficiency, the final mixture inevitably contains both assembled VLPs and unassembled coat protein (CP). Quantification of reassembly yield therefore requires two steps: (1) separation of assembled VLPs from free CP, and (2) determination of the protein concentrations in the VLP fraction and the total solution before the reassembly reaction. Among studies that report yield of reassembly, the most common approaches for this quantification are colorimetric protein assays such as bicinchoninic acid (BCA) assay; densitometric analysis of protein bands resolved by SDS–PAGE; and absorbance-based techniques such as UV–vis spectroscopy, coupled or not to liquid chromatography (*i.e.* SEC) instruments.

The BCA assay is a colorimetric, protein-specific method that quantifies protein concentration based on the reduction of Cu^{2+} to Cu^{+} by peptide bonds and thus not affected by the presence of nucleic acids. BCA assay works well for quantifying total protein. However, it is unsuitable for determining true reassembly yield if VLP reassembly is done around another encapsulated protein because it cannot distinguish between the two. We also considered densitometric analysis of SDS–PAGE bands, a semi-quantitative approach that correlates band intensity with protein concentration. Like BCA, this method is also not confounded by nucleic acids and can therefore provide informative estimates of reassembly yield when protein loading in the gel is carefully controlled. However, its utility is limited if the cargo is a protein of similar

molecular weight to the MS2 coat protein. SEC appears particularly advantageous for VLPs because it simultaneously separates assembled from unassembled particles while providing a measurement (A_{280} peak area) that correlates to capsid concentration, seemingly condensing two processes into a single procedure. However, as is true for all absorbance-based methods, the absorbance at 280 nm is influenced by cargo composition. We demonstrated this by reassembling MS2 around either luciferase RNA (~1900 nt) or a short tr-DNA (19 nt). Following nuclease digestion of unencapsulated cargo and SEC purification, both samples were brought to equal protein concentration as determined by BCA assay. When analyzed by SEC (**Figure 3A**), the luciferase RNA sample (A_{260}/A_{280} = 1.45) produced a stronger A_{280} signal than the tr-DNA sample (A_{260}/A_{280} = 1.09), despite identical protein concentrations, illustrating how cargo composition can confound absorbance-based yield quantification. In the case of this procedure, estimating the yield by comparing the absorbance of unassembled capsid with reassembled capsid would overestimate yield. Therefore, to establish a reliable correlation between A_{280} peak area and protein concentration, we recommend using the reassembled product itself as a calibrant, described in detail below.

To continue to evaluate which protein concentration method is the most suitable, we assessed the sensitivity and linear dynamic range of BCA and SDS-PAGE methods. We also included UV-Vis based methods, either coupled to SEC or not, and using either the coupled A_{280} peak area or a NanoDrop™ spectrophotometer, respectively. To this end, we expressed and purified MS2 VLPs to characterize with each method. We normalized the VLP-containing solution to A_{280} = 1, prepared dilutions spanning A_{280} values from 0.1 to 1.0, and measured each dilution using all four methods (**Supplemental Information 2**). Among them, NanoDrop™ UV–vis spectroscopy, SEC, and BCA exhibited lower coefficients of variation between technical replicates

compared to SDS-PAGE densitometry (average coefficient of variance [CV] across nonzero datapoints: $CV_{UV–Vis}$ = 0.02, CV_{SEC} = 0.008, CV_{BCA} = 0.03, $CV_{Densitometry}$ = 0.1). Moreover, the relationship between expected A_{280} values and observed measurements revealed that densitometry of SDS–PAGE dilutions had a lower coefficient of determination and higher normalized root mean square error than the other methods ($R^2_{Densitometry}$ = 0.886, R^2_{BCA} = 0.996, $R^2_{UV–Vis}$ = 0.999, R^2_{SEC} = 0.999 | $RMSE_{Densitometry}$ = 0.122, $RMSE_{BCA}$ = 0.024, $RMSE_{UV–Vis}$ = 0.012, $RMSE_{SEC}$ = 0.011). These findings reinforce that densitometry-based methods suffer from intrinsically high variability and a narrow linear dynamic range (Holzmüller & Kulozik, 2016), rendering the common practice of single-point calibration (*i.e*. using a band of known concentration to proportionally estimate the concentration of another band) unreliable. Finally, this dynamic range analysis indicates that the BCA assay does not span as broad a dynamic range as SEC coupled with A_{280} peak area. However, it remains the only tested method capable of reporting absolute protein concentration without interference from nucleic acids or other small molecules, making it a valuable complement to relative quantification approaches.

Given our findings, we propose a standardized and reproducible method for quantifying reassembly efficiency (**Figure 3B**) combining both separation of assembled and disassembled VLPs and yield quantification while addressing variability in how reassembly yield is reported in the literature. This approach allows for the calculation of either the reassembly yield alone (*Yr*) or the overall disassembly–reassembly yield (*Yg*), depending on which parameters are measured.

The core of this method involves generating a custom VLP standard specific to the VLP–cargo system under study. To do this, approximately six parallel reassembly reactions should be prepared using known amounts of coat protein and cargo in order to generate a study-specific VLP-cargo standard. After reassembly, these reactions should be pooled and subjected to centrifugation

using a 100 kDa spin filter to remove unassembled components. The resulting purified sample represents fully reassembled VLPs that serve as the reference standard. This is then analyzed by both absorbance at 280 nm (in this case, measured by SEC) and BCA assay to determine protein concentration. From these two measurements, a conversion factor (*cf*) is calculated by correlating standard protein concentration (C_S) determined by BCA with the A_{280} peak area (A_S) measured by SEC (Equation 1):

$$(Equation\ 1)\ \boldsymbol{cf} = \frac{\boldsymbol{C_S}}{\boldsymbol{A_S}}$$

Because SEC has a broad linear dynamic range, a single calibration point—run in triplicate—is sufficient. However, for added robustness, performing a short dilution series and fitting a linear regression is recommended. This calibration allows the conversion of SEC A_{280} peak areas from any experimental reassembly sample (*A*) into capsid concentration (*C*) (Equation 2):

$$(Equation\ 2)\ \boldsymbol{C} = \boldsymbol{cf} \times \boldsymbol{A}$$

Since the standard and the reassembled samples share the same coat protein and cargo composition, the calibration factor derived from this standard is directly applicable. Once the capsid concentration of the reassembled sample (*C*) is determined, the **reassembly yield** (Y_r) can be calculated using the concentration of disassembled coat protein used in the reassembly reaction (C_{CP}), the volume of disassembled coat protein used in the reassembly (V_{CP}), the volume of the reassembly reaction ($V_{reassembly}$), and the volume injected in the chromatography system ($V_{injection}$) – Equation 3:

$$(Equation\ 3)\ \boldsymbol{Y_r} = \frac{C \times V_{injection}}{C_{CP} \times V_{CP\ used\ in\ reassembly}} \times \frac{V_{reassembly}}{V_{injection}} = \frac{\boldsymbol{cf} \times \boldsymbol{A} \times \boldsymbol{V_{reassembly}}}{\boldsymbol{C_{CP}} \times \boldsymbol{V_{CP\ used\ in\ reassembly}}}$$

It is also important to consider the overall process efficiency, material losses during handling, and the practical feasibility of the method. To this end, we define the **global disassembly–reassembly yield** (*Yg*) metric, which quantifies the fraction of protein VLPs recovered relative to the initial amount subjected to disassembly. To calculate *Yg* (Equations 4 and 5), the following parameters are required: the concentration of VLPs prior to disassembly (C_{VLP}), the volume of VLP solution subjected to disassembly ($V_{VLP\ disassembled}$), and a correction factor to account for any volume changes introduced during post-disassembly purification ($V_{CP\ stock\ after\ disassembly}$ and $V_{CP\ used\ in\ reassembly}$):

$$(Equation\ 4)\ \boldsymbol{Y_g} = \frac{C \times V_{injection} \times \frac{V_{reassembly}}{V_{injection}} \times \frac{V_{CP\ stock\ after\ desalting}}{V_{CP\ used\ in\ reassembly}}}{C_{VLP} \times V_{VLP\ disassembled}}$$

$$(Equation\ 5)\ \boldsymbol{Y_g} = \frac{\boldsymbol{cf} \times \boldsymbol{A} \times \boldsymbol{V_{reassembly}} \times \frac{\boldsymbol{V_{CP\ stock\ after\ desalting}}}{\boldsymbol{V_{CP\ used\ in\ reassembly}}}}{\boldsymbol{C_{VLP}} \times \boldsymbol{V_{VLP\ disassembled}}}$$

This standardized framework enables objective, reproducible, and cargo-specific quantification of VLP reassembly, improving the comparability of results across experiments and studies. With this method in hand, it becomes possible to systematically investigate how different variables influence the final reassembly yield.

Impact of protein, crowding agent, sodium chloride concentration and buffer pH on VLP reassembly yield

Among the steps in the disassembly/reassembly process, the conditions used for reassembly vary the most. Coat protein concentration ranges from 0.05 µM of coat protein monomer (Rolfsson et al., 2008) to 146 µM (2 mg/mL) (Zhou et al., 2025). The buffer pH ranges from 5.8 (Rolfsson et al., 2008) to 8.5 (Ashley et al., 2011), but is not always reported. The sodium content in the buffer ranges from 0 (Ashley et al., 2011; Stockley et al., 2007; Sugiyama et al.,

1967) to 100 mM (Garmann et al., 2019; Glasgow et al., 2012), and some research groups add trimethylamine N-oxide (TMAO) at varying concentrations as a crowding agent (Aanei et al., 2018; Glasgow et al., 2012). The reassembly incubation temperature varies from 4 °C (Aanei et al., 2018) to 48 °C (Rolfsson et al., 2008). Reported incubation time for the reassembly reaction varies from 10 min (Williams et al., 2024) to 51 h (Zhang et al., 2015). A summary of reported reassembly conditions and the corresponding publications can be found in **Supplemental Information 1**.

To understand the impact of these variables and their interactions on reassembly yield, we estimated the effect (quantitative influence that an independent variable has on a response) by performing a full factorial 2^4 design of experiments (DOE) with a central point, in which we combinatorially tested four factors (variables) with each one assuming two levels (values). The factors and levels we adopted in the combinatorial design of experiments are coat protein monomer molarity [10 μM, 30 μM], sodium chloride molarity [0 mM, 200 mM], TMAO molarity [0 mM, 250 mM], and buffer pH [5,7]. In addition to estimating the effects, we statistically modeled yield as a function of the tested experimental conditions to predict which conditions maximize yield. The proposed model is linear and accounts for all main effects of the independent variables (x_1, x_2, x_3, x_4) as well as their two- and three-way interactions.

$$\hat{y} = b_0 + x_1 b_1 + x_2 b_2 + x_3 b_3 + x_4 b_4 + x_1 x_2 b_{12} + x_1 x_3 b_{13} + x_1 x_4 b_{14} + x_2 x_3 b_{23} + x_2 x_4 b_{24} + x_3 x_4 b_{34} + x_1 x_2 x_3 b_{123} + x_1 x_2 x_4 b_{124} + x_1 x_3 x_4 b_{134} + x_2 x_3 x_4 b_{234}$$

The modulus of the coefficients b indicates the intensity of the effect, and their signal indicates whether they have a positive or negative effect on yield. All the tested combinatorial conditions necessary for estimating the effects and generating the statistical model are represented in the experimental design matrix (**Supplemental Information 3**)

With the experimental results of the tested 17 conditions, we estimated the effects, their statistical significance (**Figure 4A**), the model parameters (**Table S3-5**), and standardized absolute effect (**Figure 4B**). Yield was quantified using the methodology developed in this study. Because the VLP standard for yield estimation was generated under the central-point condition (condition 17), yields for conditions with higher packing efficiency are likely overestimated and those with lower packing efficiency underestimated. However, this systematic bias is consistent across conditions and does not affect the interpretation of the comparative results. The interaction parameters protein-TMAO (*x1x2*), protein-TMAO-pH (*x1x2x4*), protein-NaCl-pH (*x1x3x4*) and TMAO-NaCl-pH (*x2x3x4*) are not statistically significant with a significance level $\alpha = 0.05$ and were thus removed from the proposed model. We tested the model significance by performing an ANOVA, testing the null hypothesis H_0 that all regression coefficients (except b_0) are 0. The ratio between the regression mean square and the residual mean square ($QM_R = 0.254802$, $QM_r = 0.000563$, $\underline{QM_R/QM_r = 452.93}$) was higher than a critical F-value ($\nu_1 = 10$, $\nu_2 = 40$, $\alpha = 0.05$, $\underline{F_{\nu_1,\nu_2} = 2.077}$), and the ratio of the mean square for lack of fit and the mean square for pure error ($QM_{pe} = 0.000514$, $QM_{lof} = 0.000838$, $\underline{QM_{pe}/QM_{lof} = 1.632}$) was below a critical F-value ($\nu_1 = 6$, $\nu_2 = 34$, $\alpha = 0.05$, $\underline{F_{\nu_1,\nu_2} = 2.380}$). The results of the F-tests in conjunction with a model with coefficient of determination $R^2 = 0.9912$ suggest that the model is statistically significant and adequately fits the data without significant lack of fit (**Figure 4C**).

The effect of protein concentration on the VLP reassembly yield is interconnected with other variables. While the main effect of protein concentration is one of the strongest in the model (0.232 ± 0.007, p-value = 3×10^{-27}), it also had a strong negative interaction effect with sodium chloride (-0.1189 ± 0.007, p-value = 3×10^{-15}) and a weaker negative interaction effect with pH (-0.0410 ± 0.007, p-value = 3×10^{-6}). These interaction effects indicate that the effect of protein

concentration is pronounced in certain conditions (e.g. pH 5, sodium chloride = 0 mM), but minimal in others (e.g. pH 7, sodium chloride = 200 mM) (**Figure 4D**). Conversely, sodium chloride had a consistently negative effect on reassembly, suggesting that 200 mM sodium chloride is too high of a concentration for efficient reassembly. We hypothesize that this is because elevated ionic strength disrupts the electrostatic interactions between coat proteins that are necessary for proper nucleation and propagation of capsid structures (Perlmutter, Perkett, & Hagan, 2014),. Interestingly, the magnitude of the interaction between protein concentration and sodium chloride concentration exceeds the independent effects of pH and TMAO, highlighting their comparatively greater impact on yield.

The effects of pH and the crowding agent TMAO on reassembly yield are more subtle. Within the ranges tested, these parameters produced a milder influence on reassembly yield, suggesting the reassembly process tolerates moderate pH shifts and osmolyte levels without negatively impacting reassembly yield, within the tested range. This finding complements the understanding of TMAO's impact in MS2 VLP reassembly reported by our own research group. Glasgow, Capehart, Francis, & Tullman-Ercek, 2012 reported that increasing TMAO concentration from 0 to 250 mM in reassembly reactions with 30 μM coat protein monomer, 3:5 protein monomer to cargo (tr-DNA) molar ratio, and 100 mM of sodium chloride increased the reassembly from approximately 10% to 50%. For the same coat protein monomer concentration (30 μM), sodium chloride concentration (100 mM), and pH (7), but for a coat protein monomer to tr-DNA cargo ratio of 2:1, our model predicts a reassembly yield variation from 34% to 38%. This difference suggests that the interaction between TMAO concentration and cargo concentration or protein to cargo ratio has a significant impact on reassembly yield. It is important to note that the

method utilized to estimate yield in both studies is different, highlighting the necessity of the standardized method for measuring reassembly yield developed earlier in this manuscript.

Another important outcome of the model is the absence of curvature in the response surface, which indicates that the optimal conditions for reassembly are not within the range of conditions tested here. If an optimal set of conditions had been captured within the experimental space, we would expect to see a nonlinear model with maxima. Instead, the linear behavior observed suggests that the best conditions lie outside of the ranges reported in the literature and explored to date. While it would be possible to work with higher protein and TMAO concentrations, lowering the pH below that used in this work could result in buffer conditions close to those in which the reassembled capsid is not stable. While lowering the pH may be prohibitive, the DOE results imply that the field has not yet converged on optimal reassembly parameters, and that established conditions represent only partial, rather than maximal, efficiency. Another important observation is that these experiments were performed using tr-DNA as a cargo and physicochemical interactions between the tested conditions and other cargos may vary drastically. Therefore, extrapolating the results here to other MS2 VLP-cargo systems should be done carefully and additional studies with an expanded set of variables is necessary to determine optimal conditions. Importantly, while each new cargo may require its own optimization, the present findings highlight that not all parameters will need to be reinvestigated from the underlying basics. Overall, although perfect reassembly conditions remain elusive, we identify key parameters that help guide future efforts, and the quantitative yield framework introduced here finally provides a foundation for systematic, cargo-specific optimization going forward.

Conclusion

In this study, we dissected the *in vitro* disassembly–reassembly process of MS2 VLPs to identify parameters that influence efficiency and reproducibility. We show that using a 2:1 acetic acid-to-VLP ratio at high protein concentrations with a 90-min incubation provides robust disassembly and RNA clearance. We also highlight the importance of selecting appropriate methods for buffer exchange, as trade-offs exist between protein recovery, accessibility, and processing time. Our comparison of quantification methods for reassembly yield reveals that electrophoresis and spectroscopy alone are insufficient for accurate determination; instead, we propose a standardized, cargo-specific calibration framework using HPLC-SEC coupled with BCA. Through factorial DOE analysis, we demonstrate that protein concentration is the dominant factor driving reassembly efficiency, whereas sodium chloride has a strongly negative effect, and pH and TMAO contribute more modestly. Notably, the absence of curvature in our response surfaces suggests that the optimal conditions for reassembly have not yet been defined within the literature and lie beyond the ranges typically reported.

These findings underscore two key points: (i) methodological variation has hindered progress toward reproducible, high-yield encapsulation, and (ii) the field would benefit from adopting standardized conditions and yield reporting practices. We also acknowledge the limitations of this work, which include the focus on a single type of cargo (tr-DNA) and omission of other variables such as temperature, incubation time, or different cargo-to-coat protein ratios. These variables may significantly influence assembly outcomes. Future studies expanding these parameters and testing diverse cargo will be essential for developing universally applicable guidelines. To that end, our study provides a systematic framework to improve reproducibility, comparability, and ultimately the reliability of MS2 VLPs as a versatile nanotechnology platform.

Materials and Methods

MS2 VLP expression

The strain used in this experiment is the same as that described by Robinson, Hartman, Ikwuagwu, Francis, & Tullman-Ercek, 2020. It consists of *E. coli* DH10B cells harboring the MS2 coat protein gene cloned into a pBAD33 vector. Key features of this plasmid include a chloramphenicol resistance cassette for selection and an arabinose-inducible pBAD promoter for controlled expression of the MS2 gene. Cells from a 30% glycerol stock were used to inoculate a 125 mL baffled shake flask containing 12 mL of autoclaved Lysogeny Broth (LB-Miller formulation) supplemented with 34 μg/mL chloramphenicol. Cultures were grown overnight (14–16 h) at 37 °C with shaking at 225 rpm. 10 mL of this overnight culture were used to inoculate a 2.8 L baffled shake flask containing 1 L of autoclaved LB-M medium and 1 mL of a 34 mg/mL chloramphenicol stock solution. The culture was incubated at 37 °C with shaking at 225 rpm until it reached an optical density at 600 nm (OD_{600}) of ~0.6. At this point, VLP expression was induced by adding L(+)-arabinose to a final concentration of 0.02% (w/v). The culture was incubated for an additional 16–20 h at 37 °C and 225 rpm. Cells were harvested by centrifugation at 4,800 × *g* for 10 min at 4 °C, and the supernatant was discarded. The resulting pellet was placed on ice to halt further protein expression and resuspended in 50 mL of SEC buffer (10 mM sodium phosphate, 200 mM sodium chloride, pH 7.2). If not purified immediately, cell suspension was stored at −80 °C for later use.

MS2 VLP purification

To recover and purify MS2 capsid proteins, the resuspended cell pellets were lysed using a probe sonicator (Fisher Scientific, Model FB120) set to 50% amplitude for 10 min (2-second pulses followed by 4-second intervals, for a total sonication program duration of 30 min), with samples kept on ice throughout sonication to prevent overheating. Lysates were clarified by

centrifugation at 17,000 × *g* for 10 min at 4 °C, and the pellet containing cell debris was discarded. The resulting supernatant was mixed 1:1 (v/v) with saturated ammonium sulfate aqueous solution and incubated on a vibrating platform at 4 °C for at least 2 h to precipitate protein. Following incubation, samples were centrifuged again at 17,000 × *g* for 10 min at 4 °C. The supernatant was discarded, and the resulting pellet was resuspended in 3 mL of 1× SEC buffer. To remove residual ammonium sulfate, the sample was dialyzed overnight at 4 °C using a 7,000 molecular weight cut off (MWCO) (Snakeskin) dialysis membrane against 4 L of 1× SEC buffer. The dialyzed sample was clarified by centrifugation (21,000 × *g*, 5 min, 4 °C), followed by filtration through a 0.45 µm syringe filter. For purification, the sample was subjected to Fast Protein Liquid Chromatography (FPLC) using an ÄKTA Pure system (Cytiva) equipped with a HiPrep 16/60 Sephacryl S-500 HR column, using 1x SEC buffer as the mobile phase run at a flow rate of 1 mL/min at room temperature. Up to 5 mL of sample was injected per run, and MS2 capsid elution was monitored at A_{280}, consistently appearing between 60 and 80 mL of elution volume.

High-Performance Liquid Chromatography (HPLC): VLP reassembly reactions were assessed using an HPLC system (Agilent 1260 infinity II) and an SEC column (Yara 4000, Phenomenex). The mobile phase consisted of 1 × SEC buffer (10 mM phosphate, 200 mM NaCl, pH 7.2). Runs were carried out at room temperature by injecting 100 µL of sample at the time with a total method length of 25 min. VLPs eluted between 7.7 and 9.0 min.

Transmission Electron Microscopy: 400-mesh copper grids with Formvar/carbon film (EMS P/N FCF400-Cu-50) were hydrophilized via glow discharge. We applied 10 µL of 150 nM purified capsid solution for 5 seconds, then blotted with filter paper. A 10 µL aliquot of 1% (w/v) uranyl acetate was added and immediately wicked away; this step was repeated once. A final 10 µL of

stain was applied, incubated for 4 min, and then blotted. Grids were imaged on a JEOL 1400 Flash TEM with a Gatan OneView camera.

Sodium Dodecyl Sulfate–Polyacrylamide Gel Electrophoresis (SDS-PAGE): Proteins were resolved on 12.5% polyacrylamide gels prepared with a standard Laemmli formulation. Samples were mixed with Laemmli buffer containing 10% β-mercaptoethanol, heated at 95 °C for 5 min, and loaded alongside a molecular weight ladder (EZ-run, Fisher Scientific). Electrophoresis was carried out at 150 V for ~1 h in 1× SDS running buffer until the dye front reached the bottom of the gel. Protein gels were scanned using Azure biosystems 600 and densitometry analysis was performed utilizing Fiji software (Schindelin et al., 2012).

Bicinchoninic Acid Assay. Protein concentrations were determined using the bicinchoninic acid (BCA) assay (Pierce BCA Protein Assay Kit, Thermo Scientific) according to the manufacturer's instructions, using a 96 well plate and BSA standards.

MS2 VLP disassembly and reassembly: Native MS2 VLPs (≤1 week old) were concentrated to A_{280} > 25.0 (approximately 10 mg/mL) using a 100 kDa molecular weight cutoff centrifugal filter (Amicon Ultra-15, Sigma-Aldrich) spun at 3000 × *g* in a swinging-bucket rotor. Disassembly was initiated by adding glacial acetic acid at a 2:1 (v/v) acid-to-capsid ratio, followed by incubation on ice for 1.5 h. Samples were centrifuged at 17,000 × *g* for 15 min at 4 °C to pellet residual nucleic acids. The clarified supernatant, containing disassembled capsids, was dialyzed at 4 °C against 1.5 L of chilled 1 mM acetic acid using a 3.5 kDa molecular weight cutoff dialysis cassette. Dialysis was performed in two steps: 3 h in fresh buffer, followed by overnight dialysis. Successful RNA removal was confirmed by an A_{260}/A_{280} absorbance ratio of ~0.6. Reassembly conditions were varied as noted in the results section. In all cases, water, buffer, salt, crowding agent, cargo, and protein were added at listed concentrations in the order listed here, and incubated for 48 h at 4 °C.

The samples were centrifuged at 17,000 × g for 15 min and supernatant collected for further analysis.

Supplementary material description

Supplemental Information 1 summarizes literature on MS2 VLP disassembly/reassembly conditions. Supplemental Information 2 compares linearity across protein quantification methods. Supplemental Information 3 provides supporting calculations for statistical design of experiments using reassembly yield as the response. Supplemental Information 4 contains raw data and results of statistical design of experiments using A_{260}/A_{280} as the response.

Acknowledgements

This work was supported by the National Science Foundation (CBET-2043973, to D.T.-E.). D.C.A. received support from the Chemistry of Life Processes Predoctoral Training Program at Northwestern University (NIH T32GM149439). M.M.M. was supported in part by the Northwestern University Graduate School Cluster in Biotechnology, Systems, and Synthetic Biology, which is affiliated with the Biotechnology Training Program. S.L. was partially supported by the Molecular Biophysics Training Program at Northwestern University (NIH 5T32GM140995-04). A.C.C. was supported by Conselho Nacional de Desenvolvimento Científico e Tecnológico (CNPq grant number 303063/2022-0). N.W.K. was supported by the U.S. Army Research Office (W52P1J-21-9-3023 P00003/CS-21-0701-001).

Author's Contributions (CRediT)

D.C.A.: Conceptualization (lead), methodology (lead), validation (lead), formal analysis (equal), investigation (equal), resources (supporting), data curation (lead), writing – original draft (lead); writing – review and edit (supporting), visualization (lead), project administration (equal), funding acquisition (supporting). **E.S.V.:** validation (supporting), formal analysis (supporting),

investigation (equal), visualization (support). **M.M.M.:** investigation (supporting), data curation (supporting) **S.L.:** investigation (supporting) **C.E.M.:** writing – review and edit (equal) **A.C.C.:** formal analysis (equal), data curation (supporting) **N.W.K.:** writing – review and edit (equal), visualization (supporting) **D.T.-E.:** writing – review and edit (equal), project administration (equal), funding acquisition (lead).

References

Aanei, I. L., Glasgow, J. E., Capehart, S. L., & Francis, M. B. (2018). Encapsulation of Negatively Charged Cargo in MS2 Viral Capsids. In C. Wege & G. P. Lomonossoff (Eds.), *Virus-Derived Nanoparticles for Advanced Technologies: Methods and Protocols* (pp. 303–317). New York, NY: Springer. doi: 10.1007/978-1-4939-7808-3_21

Ashley, C. E., Carnes, E. C., Phillips, G. K., Durfee, P. N., Buley, M. D., Lino, C. A., Padilla, D. P., Phillips, B., Carter, M. B., Willman, C. L., Brinker, C. J., Caldeira, J. C., Chackerian, B., Wharton, W., & Peabody, D. S. (2011). Cell-Specific Delivery of Diverse Cargos by Bacteriophage MS2 Virus-like Particles. *ACS Nano*, *5*(7), 5729–5745. doi: 10.1021/nn201397z

A. Williams, L., Neophytou, A., F. Garmann, R., Chakrabarti, D., & N. Manoharan, V. (2024). *Effect of coat-protein concentration on the self-assembly of bacteriophage MS2 capsids around RNA*. doi: 10.1039/D3NR03292B

Callanan, J., Stockdale, S. R., Adriaenssens, E. M., Kuhn, J. H., Rumnieks, J., Pallen, M. J., Shkoporov, A. N., Draper, L. A., Ross, R. P., & Hill, C. (2021). Leviviricetes: Expanding and restructuring the taxonomy of bacteria-infecting single-stranded RNA viruses. *Microbial Genomics*, *7*(11), 000686. doi: 10.1099/mgen.0.000686

Frietze, K. M., Peabody, D. S., & Chackerian, B. (2016). Engineering virus-like particles as vaccine platforms. *Current Opinion in Virology*, *18*, 44–49. doi: 10.1016/j.coviro.2016.03.001

Fu, Y., & Li, J. (2016). A novel delivery platform based on Bacteriophage MS2 virus-like particles. *Virus Research*, *211*, 9–16. doi: 10.1016/j.virusres.2015.08.022

Garmann, R. F., Goldfain, A. M., & Manoharan, V. N. (2019). Measurements of the self-assembly kinetics of individual viral capsids around their RNA genome. *Proceedings of the National Academy of Sciences*, *116*(45), 22485–22490. doi: 10.1073/pnas.1909223116

Glasgow, J. E., Capehart, S. L., Francis, M. B., & Tullman-Ercek, D. (2012). Osmolyte-Mediated Encapsulation of Proteins inside MS2 Viral Capsids. *ACS Nano*, *6*(10), 8658–8664. doi: 10.1021/nn302183h

Golmohammadi, R., Valegård, K., Fridborg, K., & Liljas, L. (1993). The refined structure of bacteriophage MS2 at 2.8 A resolution. *Journal of Molecular Biology*, *234*(3), 620–639. doi: 10.1006/jmbi.1993.1616

Hartman, E. C., Jakobson, C. M., Favor, A. H., Lobba, M. J., Álvarez-Benedicto, E., Francis, M. B., & Tullman-Ercek, D. (2018). Quantitative characterization of all single amino acid variants of a viral capsid-based drug delivery vehicle. *Nature Communications*, *9*(1). doi: 10.1038/s41467-018-03783-y

Ikwuagwu, B., & Tullman-Ercek, D. (2022). Virus-like particles for drug delivery: A review of methods and applications. *Current Opinion in Biotechnology*, *78*, 102785. doi: 10.1016/j.copbio.2022.102785

Liang, S., Butaney, K., de Castro Assumpção, D., Jung, J., Kennedy, N. W., & Tullman-Ercek, D. (2025). Synthetic Rewiring of Virus-like Particles via Circular Permutation Enables Modular Peptide Display and Protein Encapsulation. *ACS Nano, 18;19(45):39168-80*, 102785. doi: 10.1021/acsnano.5c12293

Neto, B. B., Scarminio, I. S., & Bruns, R. E. (2010). *Como Fazer Experimentos—4.ed.: Pesquisa e Desenvolvimento na Ciência e na Indústria*. Bookman. Retrieved from https://books.google.com/books?id=FDnT9ygeOccC

Pasloske, B. L., Walkerpeach, C. R., Obermoeller, R. D., Winkler, M., & DuBois, D. B. (1998). Armored RNA technology for production of ribonuclease-resistant viral RNA controls and standards. *Journal of Clinical Microbiology*, *36*(12), 3590–3594. doi: 10.1128/JCM.36.12.3590-3594.1998

Perlmutter, J. D., Perkett, M. R., & Hagan, M. F. (2014). Pathways for virus assembly around nucleic acids. *Journal of Molecular Biology*, *426*(18), 3148–3165. doi: 10.1016/j.jmb.2014.07.004

Robinson, S. A., Hartman, E. C., Ikwuagwu, B. C., Francis, M. B., & Tullman-Ercek, D. (2020). Engineering a Virus-like Particle to Display Peptide Insertions Using an Apparent Fitness Landscape. *Biomacromolecules*, *21*(10), 4194–4204. doi: 10.1021/acs.biomac.0c00987

Rolfsson, O., Toropova, K., Morton, V., Francese, S., Basnak, G., Thompson, G. S., Homans, S. W., Ashcroft, A. E., Stonehouse, N. J., Ranson, N. A., & Stockley, P. G. (2008). RNA packing specificity and folding during assembly of the bacteriophage MS2. *Computational and Mathematical Methods in Medicine*, *9*(3–4), 339–349. doi: 10.1080/17486700802168445

Schindelin, J., Arganda-Carreras, I., Frise, E., Kaynig, V., Longair, M., Pietzsch, T., Preibisch, S., Rueden, C., Saalfeld, S., Schmid, B., Tinevez, J.-Y., White, D. J., Hartenstein, V., Eliceiri, K., Tomancak, P., & Cardona, A. (2012). Fiji: An open-source platform for biological-image analysis. *Nature Methods*, *9*(7), 676–682. doi: 10.1038/nmeth.2019

Stockley, P. G., Rolfsson, O., Thompson, G. S., Basnak, G., Francese, S., Stonehouse, N. J., Homans, S. W., & Ashcroft, A. E. (2007). A Simple, RNA-Mediated Allosteric Switch Controls the Pathway to Formation of a T=3 Viral Capsid. *Journal of Molecular Biology*, *369*(2), 541–552. doi: 10.1016/j.jmb.2007.03.020

Strauss, J. H., & Sinsheimer, R. L. (1963). Purification and properties of bacteriophage MS2 and of its ribonucleic acid. *Journal of Molecular Biology*, *7*(1), 43–54. doi: 10.1016/S0022-2836(63)80017-0

Sugiyama, T., Hebert, R. R., & Hartman, K. A. (1967). Ribonucleoprotein complexes formed between bacteriophage MS2 RNA and MS2 Protein *in vitro*. *Journal of Molecular Biology*, *25*(3), 455–463. doi: 10.1016/0022-2836(67)90198-2

Szyszka, T. N., Siddiquee, R., Loustau, A., Adamson, L. S. R., Rennie, C., Huang, T., Young, R., Care, A., & Lau, Y. H. (2025). High-Fidelity In Vitro Packaging of Diverse Synthetic Cargo into Encapsulin Protein Cages. *Angewandte Chemie International Edition*, *64*(23), e202422459. doi: 10.1002/anie.202422459

Wu, M., Brown, W. L., & Stockley, P. G. (1995). Cell-specific delivery of bacteriophage-encapsidated ricin A chain. *Bioconjugate Chemistry*, *6*(5), 587–595. doi: 10.1021/bc00035a013

Yang, M., Rao, G., Li, L., Qi, L., Ma, C., Zhang, H., Gong, J., Wei, B., Zhang, X.-E., Chen, G., *Cao, S.*, & Li, F. (2024). Transformation of a Viral Capsid from Nanocages to Nanotubes

and Then to Hydrogels: Redirected Self-Assembly and Effects on Immunogenicity. *ACS Nano*, *18*(21), 13755–13767. doi: 10.1021/acsnano.4c01969

Zhang, L., Sun, Y., Chang, L., Jia, T., Wang, G., Zhang, R., Zhang, K., & Li, J. (2015). A novel method to produce armored double-stranded DNA by encapsulation of MS2 viral capsids. *Applied Microbiology and Biotechnology*, *99*(17), 7047–7057. doi: 10.1007/s00253-015-6664-4

Zhou, W., Ma, S., Gao, R., Tang, Y., Zhang, H., Liang, A., Yang, M., Ma, C., Fan, Q., *Zhang, X.-E.*, & Li, F.* (2025). Assembly of Matryoshka-Type Protein Nanocages for Compartmentalized Oxygen Sensing. *Nano Letters*, *25*(11), 4433–4440. doi: 10.1021/acs.nanolett.4c06699

Figures (artwork)

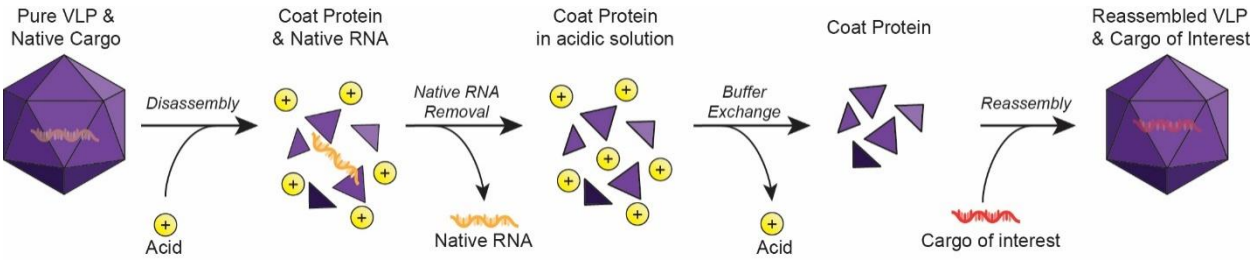

Figure 1: Overall process for encapsulating a cargo of interest in MS2 VLPs. Biologically produced and purified MS2 VLPs are first incubated under acidic conditions to induce capsid disassembly and precipitate nucleic acids natively packed during VLP expression. The precipitated nucleic acids are removed by centrifugation, and the resulting coat protein solution is buffer exchanged to eliminate excess acid and adjust the pH. Finally, the coat proteins are incubated with the cargo of interest in buffer, promoting spontaneous self-assembly and encapsulation of cargo with total or local negative charges on its structure.

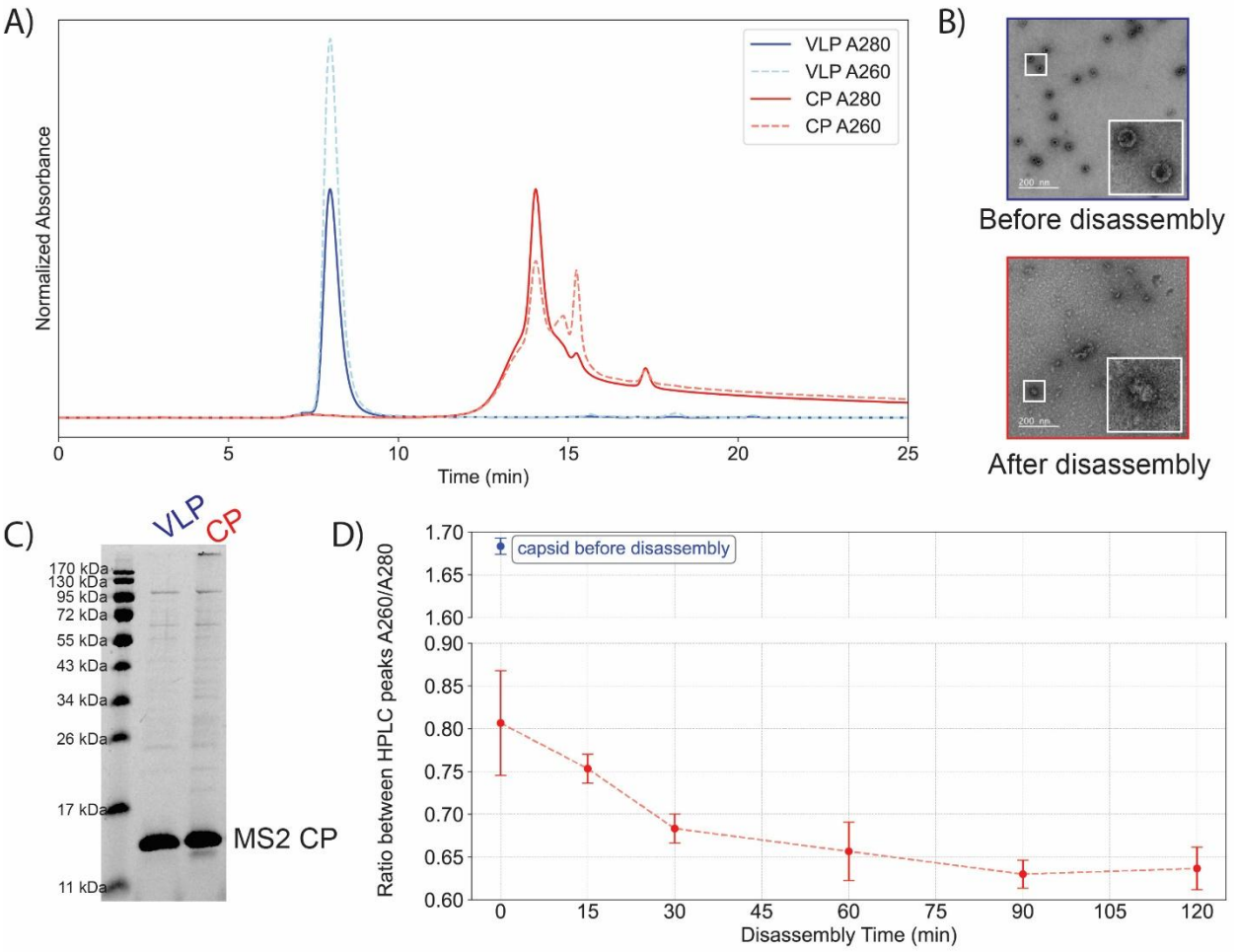

610

611 **Figure 2:** Characterization of MS2 VLP disassembly following acid treatment. **A)** Size exclusion
612 chromatography (SEC) traces showing a shift in retention time before (labelled "VLP") and after
613 (labelled "CP") incubation with acetic acid, indicating capsid disassembly. A concurrent decrease
614 in A_{260} absorbance reflects the removal of native nucleic acid via precipitation and centrifugation.
615 **B)** Transmission electron microscopy (TEM) images of VLPs before and after acid incubation,
616 demonstrating the transition from intact capsids to irregular protein aggregates. **C)** SDS-PAGE of
617 samples before and after disassembly in acetic acid indicating that protein does not degrade during
618 disassembly **D)** A_{260}/A_{280} absorbance ratio of the protein solution as a function of incubation time,
619 showing that RNA removal improves with longer incubation and reaches a plateau after ~90 min.

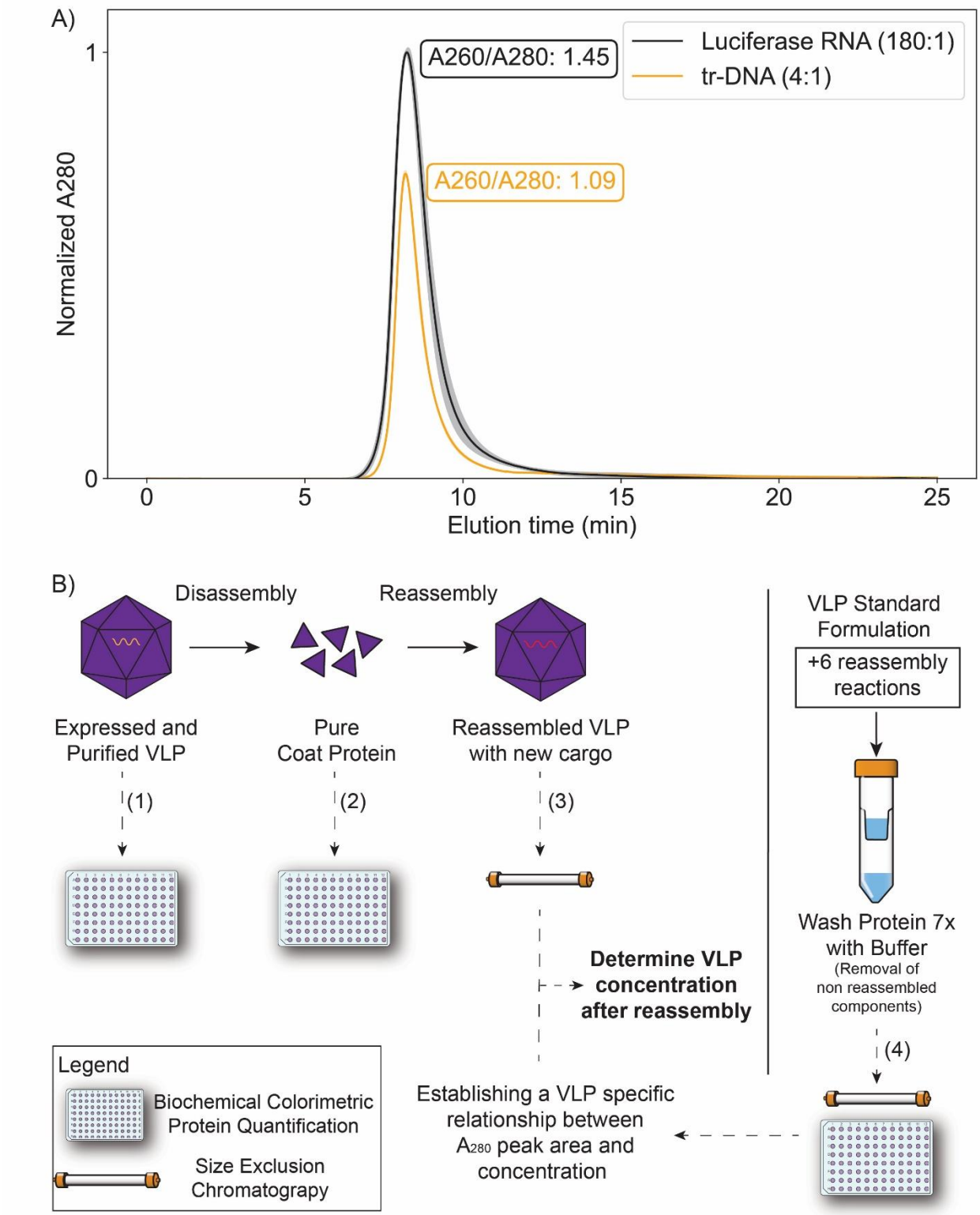

Figure 3: A) SEC chromatograms normalized by A_{280} of two samples containing different nucleic acid-based cargos (varying in amount and nature) but with identical protein concentrations as

measured by BCA. The resulting differences in absorbance highlight the interference caused by cargo. **B)** Schematic of the proposed method for quantifying VLP reassembly yield. The concentrations of the purified VLP (1) and the disassembled capsid (2) are determined using the BCA assay. The reassembly reaction product is analyzed by SEC (3). Additional reassembly reactions are performed to generate a standard curve relating SEC peak area to concentration (4). This standard is then used to convert the SEC peak area of the experimental reassembly product into concentration, enabling calculation of reassembly yield.

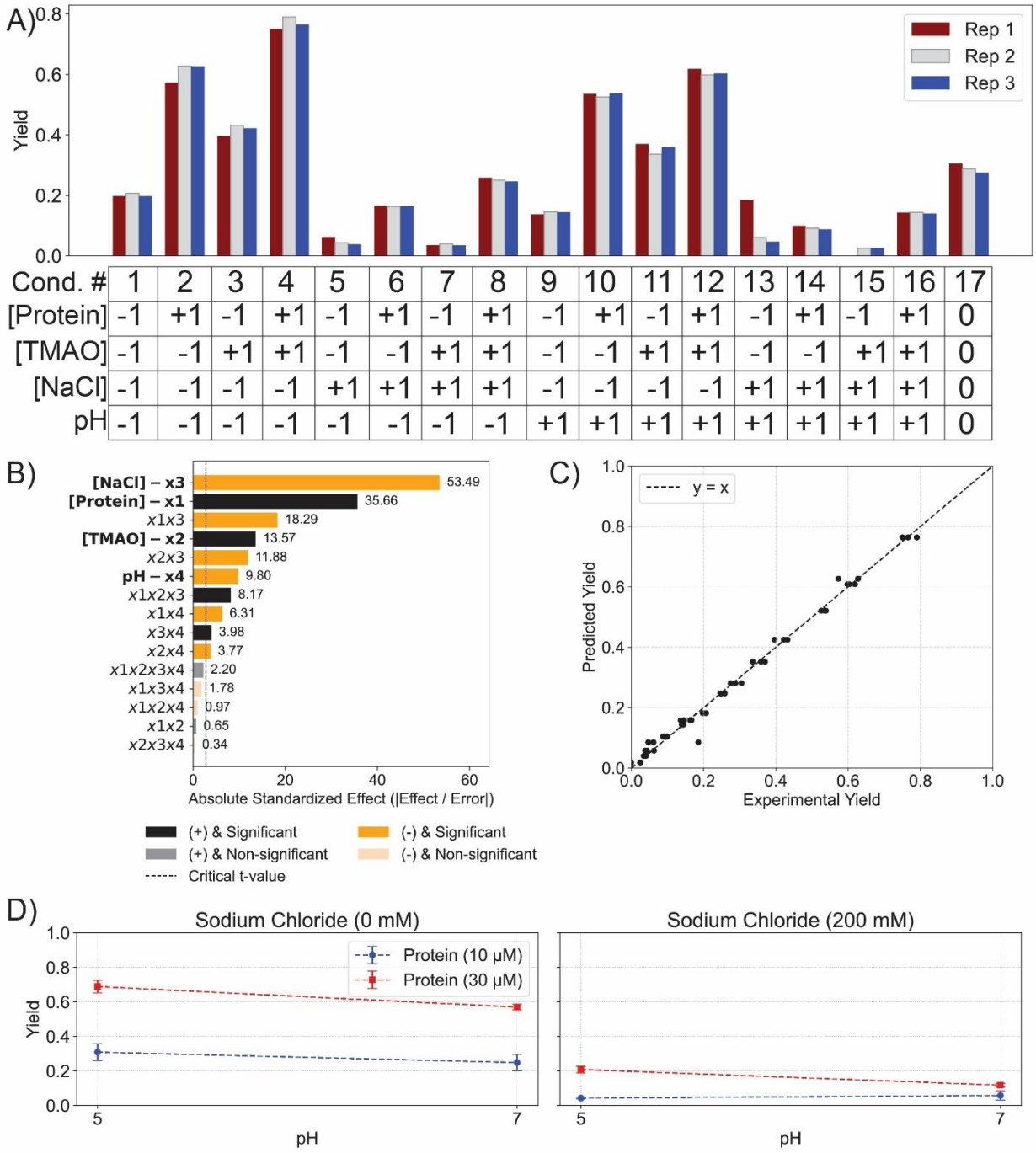

Cond. #	1	2	3	4	5	6	7	8	9	10	11	12	13	14	15	16	17
[Protein]	-1	+1	-1	+1	-1	+1	-1	+1	-1	+1	-1	+1	-1	+1	-1	+1	0
[TMAO]	-1	-1	+1	+1	-1	-1	+1	+1	-1	-1	+1	+1	-1	-1	+1	+1	0
[NaCl]	-1	-1	-1	-1	+1	+1	+1	+1	-1	-1	-1	-1	+1	+1	+1	+1	0
pH	-1	-1	-1	-1	-1	-1	-1	-1	+1	+1	+1	+1	+1	+1	+1	+1	0

Figure 4. A) Reassembly yield for each individual replicate of each tested condition. **B)** Pareto chart of standardized effects showing the influence of individual factors and their interactions on yield. The vertical dashed line represents the critical *t*-value for statistical significance. **C)** Experimental versus predicted yield from the fitted model. Each point represents one replicate.

The dashed line corresponds to the ideal fit ($y = x$), indicating strong agreement between experimental data and model predictions. **D)** Marginal means plot indicating the impact of protein molarity, sodium chloride molarity, and pH and their interactions on reassembly yield